Monthly Notices
of the
ROYAL ASTRONOMICAL SOCIETY

MNRAS **462,** 740–750 (2016)
Advance Access publication 2016 July 11

doi:10.1093/mnras/stw1662

Pseudo-heteroclinic connections between bicircular restricted four-body problems

Esther Barrabés,[1]★ Gerard Gómez,[2] Josep M. Mondelo[3] and Mercé Ollè[4]★

[1]*Departament de Informàtica, Matemàtica Aplicada i Estadística, Universitat de Girona, E-17071 Girona, Spain*
[2]*IEEC & Departament de Matemàtiques i Informàtica, Universitat de Barcelona, Gran Via 585, E-08007 Barcelona, Spain*
[3]*IEEC & Departament de Matemàtiques, Universitat Autònoma de Barcelona, E-08193 Bellaterra, Spain*
[4]*Departament de Matemàtiques, Universitat Politècnica de Catalunya, Av. Diagonal 647, E-08028 Barcelona, Spain*

Accepted 2016 July 7. Received 2016 July 4; in original form 2016 April 27

ABSTRACT

In this paper, we show a mechanism to explain transport from the outer to the inner Solar system. Such a mechanism is based on dynamical systems theory. More concretely, we consider a sequence of uncoupled bicircular restricted four-body problems – BR4BP – (involving the Sun, Jupiter, a planet and an infinitesimal mass), being the planet Neptune, Uranus and Saturn. For each BR4BP, we compute the dynamical substitutes of the collinear equilibrium points of the corresponding restricted three-body problem (Sun, planet and infinitesimal mass), which become periodic orbits. These periodic orbits are unstable, and the role that their invariant manifolds play in relation with transport from exterior planets to the inner ones is discussed.

Key words: methods: numerical – celestial mechanics – planets and satellites: dynamical evolution and stability.

1 INTRODUCTION

The geometrical approach provided by dynamical systems methods allows the use of stable/unstable manifolds for the determination of spacecraft transfer orbits in the Solar system (see for example, Gómez et al. 1993; Bollt & Meiss 1995). The same kind of methods can also be used to explain some mass transport mechanisms in the Solar system.

Inspired by the work of Gladman et al. (1996), Ren et al. (2012) introduced two natural mass transport mechanisms in the Solar system between the neighbourhoods of Mars and the Earth. The first mechanism is a short-time transport, and is based on the existence of 'pseudo-heteroclinic' connections between libration point orbits of uncoupled pairs of Sun–Mars and Sun–Earth circular restricted three-body problems, RTBPs. The term 'pseudo' is due to the fact that the two RTBPs are uncoupled, the hyperbolic manifolds of the departing and arrival RTBP only intersect in configuration space and a small velocity increment is required to switch from one to the other. The second and long-time transport mechanism relies on the existence of heteroclinic connections between long-period periodic orbits in one single RTBP (the Sun–Jupiter system), and is the result of the strongly chaotic motion of the minor body of the problem.

Lo & Ross (1999) also explored the transport mechanism by considering a sequence of RTBP. In each of them, they computed the osculating orbital elements of the one-dimensional invariant manifolds of the collinear libration points L_1 and L_2 (see Fig. 1). The results suggest possible heteroclinic connections between the manifolds associated with the three most outer planets.

Collisions in the Solar system are abundant and are a mechanism that changes the velocity of the colliding bodies. After a collision, the bodies can, eventually, be injected in a suitable invariant manifold that transports them from their original location to very distant places. This possibility has not been explored in this paper.

The present paper is devoted to provide a dynamical mechanism for the transport of comets, asteroids and small particles from the outer towards the inner Solar system. The study is based on the analysis of the dynamics of the bicircular restricted four-body problem (BR4BP) in which the main bodies (primaries) are the Sun, Jupiter and an external planet (Saturn, Uranus and Neptune); in this way, the outer Solar system will be modelled as a sequence of bicircular models. Some preliminary results about this problem already appeared in Ollé et al. (2015).

The BR4BP is a simplified model of the four-body problem, in which it is assumed that a particle moves under the gravitational attraction of two bodies (primaries) revolving in circular orbits around their centre of mass, and a third primary, moving in a circular orbit around their barycentre. We will consider as primaries the Sun and two planets, and assume that the four bodies move in the same plane. In contrast with the RTBP, this model is not coherent, in the sense that the circular trajectories assumed for the Sun and the two planets do not satisfy Newton's equations of the three-body problem. The lack of coherence becomes an important issue when there are resonances between the natural motion of the infinitesimal particle and the period of the third primary, as was shown by Andreu (1998) in the Sun–Earth–Moon system, but this is not the case for the problem under consideration.

★ E-mail: barrabes@ima.udg.es (EB); merce.olle@upc.edu (MO)

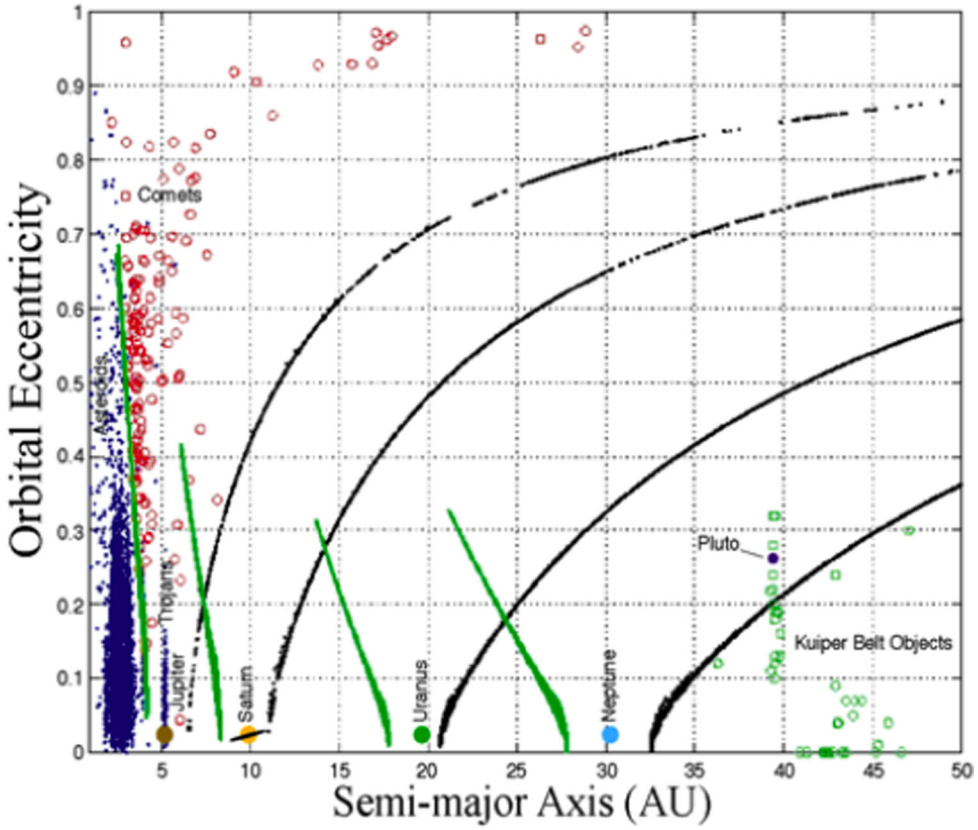

Figure 1. Semimajor axis and eccentricity of the stable manifold of the L_2 libration point (right-hand side of each planet, curves towards the right) and of the unstable manifold of the L_1 libration point (left-hand side of each planet, curves towards the left) for several Sun–planet systems modelled as circular restricted three-body problems (Lo & Ross 1999).

The differential equations of the BR4BP are non-autonomous, with periodic time dependence with the same period as the synodical period of the planet. The time-periodic character of the differential equations implies the non-existence of equilibrium points. Nevertheless, the BR4BP can be viewed as a perturbation of the RTBP, where equilibrium points do exist. The collinear equilibrium points, L_i, $i = 1, 2, 3$, are replaced by some periodic orbits that are named their *dynamical substitutes*, since they play in the BR4BP a dynamic role similar to the one of the equilibrium points.

We will consider bicircular models Sun–planet–planet. According to the values of the gravity potential of the planets (see Fig. 2), it is convenient to include Jupiter in all the BR4BPs. As has already been said, the Solar system will be modelled by a sequence of bicircular Sun–Jupiter–planet problems, dynamically uncoupled. Taking an aligned initial configuration of the three primaries, for each BR4BP, the dynamical substitutes of L_1 and L_2 corresponding to the (Sun+Jupiter)–planet system can be computed. These periodic orbits inherit the centre $\times$ saddle character of their associated equilibrium points. The hyperbolic invariant stable and unstable manifolds associated with the dynamical substitutes will be used to determine the possible pseudo-heteroclinic connections between the different BR4BPs, analogously as it was done by Lo & Ross (1999).

The paper is organized as follows.

(i) Section 2 introduces the methodology for the computation of periodic orbits, and their hyperbolic invariant manifolds, in time-periodic differential systems. Some lemmas supporting the statements of this section are given in Appendix A.

(ii) In Section 3, the differential equations of the bicircular problem, together with the numerical values of the parameters appearing in the equations, are given. Using the methods introduced in the preceding section, the dynamical substitutes of the equilibrium points are computed for the different BC4BPs used in the paper.

(iii) Section 4 is devoted to the computation of the invariant manifolds of the substitutes of the equilibrium points in the bicircular four-body problems: Sun–Jupiter–Neptune, Sun–Jupiter–Uranus and Sun–Jupiter–Saturn. The possible connections between the invariant manifolds of these problems for moderate ranges of time integration are analysed in this last section.

2 COMPUTING PERIODIC ORBITS AND THEIR INVARIANT MANIFOLDS IN PERIODIC DIFFERENTIAL SYSTEMS

The general form of a time-periodic system of (first-order) differential equations is

$$\dot{\boldsymbol{x}} = \boldsymbol{f}(\boldsymbol{x}, \theta_0 + t\omega), \tag{1}$$

where $\boldsymbol{x} \in \mathbb{R}^n$, t is the independent variable, $\theta_0, \omega \in \mathbb{R}$ and

$$\boldsymbol{f} : \mathbb{R}^n \times \mathbb{R} \longrightarrow \mathbb{R}$$
$$(\boldsymbol{x}, \theta) \longmapsto \boldsymbol{f}(\boldsymbol{x}, \theta)$$

is 2π-periodic in θ. This is a time-periodic differential system with period $T = 2\pi/\omega$. Actually, it is a family of systems of ordinary differential equations (ODE) depending on the parameter θ_0. For

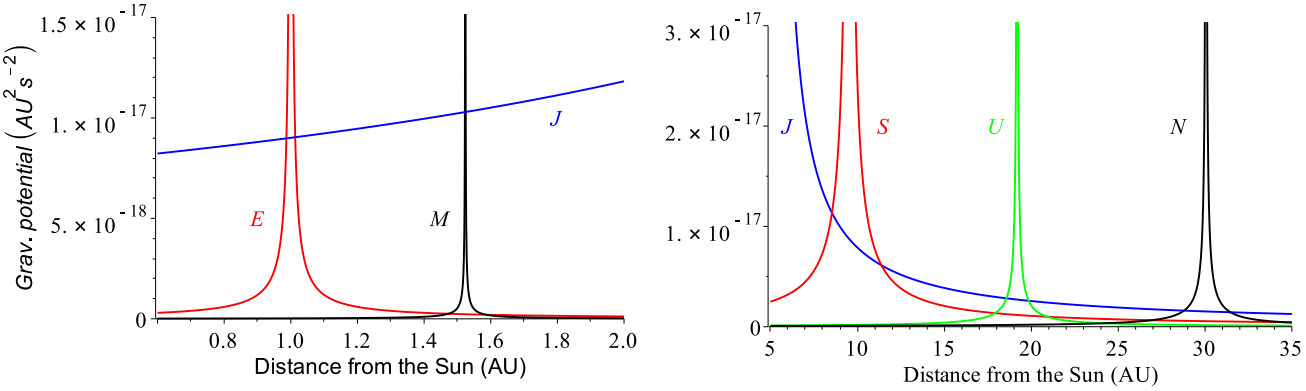

Figure 2. Values of the gravity potential (in au^2 s^{-2}) of the Earth (E), Mars (M) and Jupiter (J) in the heliocentric region including the orbits of the Earth and Mars (left), and gravity potential of Jupiter (J), Saturn (S), Uranus (U) and Neptune (N) in the heliocentric region corresponding to the outer Solar system.

each value of θ_0, we will denote by $\boldsymbol{\phi}_t^{\theta_0}$ the flow from time 0 to time t of the corresponding system of ODE, this is

$$\begin{cases} \frac{\mathrm{d}}{\mathrm{d}t}\boldsymbol{\phi}_t^{\theta_0} = \boldsymbol{f}\left(\boldsymbol{\phi}_t^{\theta_0}(\boldsymbol{x}_0), \theta_0 + t\omega\right), \\ \boldsymbol{\phi}_0^{\theta_0}(\boldsymbol{x}_0) = \boldsymbol{x}_0. \end{cases} \tag{2}$$

For a fixed θ_0, the flow $\boldsymbol{\phi}_t^{\theta_0}(x_0)$ can be evaluated as a function of $t, \boldsymbol{x}_0$ using a numerical integrator of ODE. The flows corresponding to the different possible values of θ_0 are related by the following lemma.

Lemma 1 *For any $\boldsymbol{x} \in \mathbb{R}^n$, $\theta, t, s \in \mathbb{R}$, we have*

$$\boldsymbol{\phi}_s^{\theta+t\omega}\left(\boldsymbol{\phi}_t^{\theta}(\boldsymbol{x})\right) = \boldsymbol{\phi}_{s+t}^{\theta}(\boldsymbol{x}).$$

Proof: Introducing θ as an additional coordinate makes autonomous the system of ODE (1) as

$$\begin{cases} \dot{\boldsymbol{x}} = \boldsymbol{f}(\boldsymbol{x}, \theta), \\ \dot{\theta} = \omega. \end{cases}$$

Denote this last system as $\dot{\boldsymbol{X}} = \boldsymbol{F}(\boldsymbol{X})$, with $\boldsymbol{X} = (\boldsymbol{x}, \theta)^\top$ and $\boldsymbol{F}(\boldsymbol{X}) = (\boldsymbol{f}(\boldsymbol{x}, \theta), \omega)^\top$. Denote its flow from time 0 to time t by $\boldsymbol{\Phi}_t$. The components of $\boldsymbol{\Phi}_t$ are

$$\boldsymbol{\Phi}_t(\boldsymbol{X}) = \begin{pmatrix} \boldsymbol{\phi}_t^{\theta}(\boldsymbol{x}) \\ \theta + t\omega \end{pmatrix},$$

with $\boldsymbol{\phi}_t^{\theta}$ defined by equation (2). Now, for any $\boldsymbol{X} = (\boldsymbol{x}, \theta)^\top$, by the flow property of $\boldsymbol{\Phi}_t$,

$$\begin{pmatrix} \boldsymbol{\phi}_{s+t}^{\theta}(\boldsymbol{x}_0) \\ \theta + (s+t)\omega \end{pmatrix} = \boldsymbol{\Phi}_{s+t}(\boldsymbol{X}) = \boldsymbol{\Phi}_s\left(\boldsymbol{\Phi}_t(\boldsymbol{X})\right)$$
$$= \boldsymbol{\Phi}_s\begin{pmatrix} \boldsymbol{\phi}_t^{\theta}(\boldsymbol{x}) \\ \theta + t\omega \end{pmatrix} = \begin{pmatrix} \boldsymbol{\phi}_s^{\theta+t\omega}\left(\boldsymbol{\phi}_t^{\theta}(\boldsymbol{x})\right) \\ \theta + t\omega + s\omega \end{pmatrix},$$

and the lemma follows from the equality of the first components in both ends. □

Assume that, given a starting phase θ_0, we have found an initial condition $\boldsymbol{x}_0 \in \mathbb{R}^n$ of a T-periodic orbit of system (1) by numerically solving for $\boldsymbol{x}_0$ the equation

$$\boldsymbol{\phi}_T^{\theta_0}(\boldsymbol{x}_0) = \boldsymbol{x}_0. \tag{3}$$

Once $\boldsymbol{x}_0$ is found (for the starting phase θ_0), a numerically computable parametrization of the periodic orbit is provided by the function $\boldsymbol{\varphi}$ defined as

$$\boldsymbol{\varphi}(\theta) = \boldsymbol{\phi}_{(\theta-\theta_0)/\omega}^{\theta_0}(\boldsymbol{x}_0). \tag{4}$$

Using Lemma 1, $\boldsymbol{\varphi}$ can be shown (see Lemma 2 in Appendix A) to be 2π-periodic in θ and to satisfy the invariance equation

$$\boldsymbol{\phi}_t^{\theta}(\boldsymbol{\varphi}(\theta)) = \boldsymbol{\varphi}(\theta + t\omega). \tag{5}$$

Finding a periodic orbit in terms of an initial condition $\boldsymbol{x}_0$ requires choosing a starting phase θ_0 to be used in its computation. But the periodic orbit itself, as an invariant object, is independent of θ_0. This is suggested by the previous invariance equation (5) and further corroborated by the following fact: by a straightforward application of Lemma 1, it can be checked that if $\boldsymbol{x}_1 = \boldsymbol{\phi}_t^{\theta_0}(\boldsymbol{x}_0)$ and $\theta_1 = \theta_0 + t\omega$, then

$$\boldsymbol{\phi}_{(\theta-\theta_0)/\omega}^{\theta_0}(\boldsymbol{x}_0) = \boldsymbol{\phi}_{(\theta-\theta_1)/\omega}^{\theta_1}(\boldsymbol{x}_1).$$

An additional way to see that the periodic orbit, as invariant object, is independent of θ_0 is to check, again through Lemma 1, that $\boldsymbol{\varphi}(\theta)$ is a periodic orbit of the 2π-periodic differential system

$$\boldsymbol{x}'(\theta) = \frac{1}{\omega}\boldsymbol{f}\left(\boldsymbol{x}(\theta), \theta\right),$$

which is obtained from equation (1) by changing the independent variable to θ. Actually, the BR4BP could be defined as a 2π-periodic system in this way (using θ as time), thus avoiding the need for θ_0. We will not use this last approach since we will work with different BR4BP models and we will want to refer all of them to the same time-scale.

Assume now that $\boldsymbol{x}_0$ is an initial condition of a periodic orbit of equation (1) with starting phase θ_0, found by solving equation (3), and assume also that $D\boldsymbol{\phi}_T^{\theta_0}(\boldsymbol{x}_0)$ (its monodromy matrix) has an eigenvalue $\Lambda \in \mathbb{R}$, $\Lambda > 1$ (resp. $\Lambda < 1$), with eigenvector $\boldsymbol{v}_0$. In order to state a formula for the linear approximation of the corresponding unstable (resp. stable) manifold of the periodic orbit, we first define

$$\boldsymbol{v}(\theta) = \Lambda^{-\frac{\theta-\theta_0}{2\pi}} D\boldsymbol{\phi}_{(\theta-\theta_0)/\omega}(\boldsymbol{x}_0)\boldsymbol{v}_0. \tag{6}$$

Again using Lemma 1 (see Lemma 3), $\boldsymbol{v}$ can be shown to be a 2π-periodic function of θ. The linear approximation of the corresponding invariant manifold is given by

$$\bar{\boldsymbol{\psi}}(\theta, \xi) = \boldsymbol{\phi}(\theta) \pm \xi\boldsymbol{v}(\theta). \tag{7}$$

According to the sign + or −, in the previous expression, we will talk about the two branches (positive and negative) of the invariant manifold, that will be usually denoted by W_+ and W_-, respectively. The fact that equation (7) provides the linear approximation (in ξ) of an invariant manifold of the periodic orbit is given by the following

approximate invariance equation, that can be proven again through Lemma 1 (see Lemma 4):

$$\boldsymbol{\phi}_t^{\theta}\left(\bar{\boldsymbol{\psi}}(\theta,\xi)\right) = \bar{\psi}\left(\theta + t\omega, \Lambda^{t/T}\xi\right) + O(\xi^2). \tag{8}$$

In the computations that follow, we will generate points on a periodic orbit with initial condition $\boldsymbol{x}_0$ for the starting phase θ_0 by numerically evaluating $\boldsymbol{\varphi}(\theta)$ as defined in equation (4) for different values of θ. For any of such values, the corresponding trajectory in the invariant manifold (corresponding to the Λ eigenvalue of the monodromy matrix) will be obtained by choosing ξ small enough for the $O(\xi^2)$ term in equation (8) to be small (e.g. $\xi = 10^{-6}$) and numerically evaluating

$$\boldsymbol{\phi}_t^{\theta}\left(\bar{\boldsymbol{\psi}}(\theta,\xi)\right),$$

for t as large as needed.

3 THE BICIRCULAR PROBLEM

3.1 The equations of motion

The BR4BP is a simplified model for the four-body problem. We assume that two primaries are revolving in circular orbits around their centre of mass, assumed from now on to be the origin O, and a third primary moves in a circular orbit around this origin. The BR4BP describes the motion of a massless particle that moves under the gravitational attraction of the three primaries without affecting them. We consider here the planar case, in which all the bodies move in the same plane.

As mentioned in the introduction, we will assume that the two main primaries are the Sun and Jupiter, and the third one a planet of the outer Solar system. Our aim is to consider the Solar system as a sequence of *uncoupled* bicircular models in order to get a first insight of transport in the Solar system that may be explained using the *separated* bicircular problems.

First, and in order to fix the notation, we briefly recall how to obtain the equations of motion of the BR4BP (see also Andreu 1998).

Consider a reference system centred at the centre of mass of the Sun–Jupiter system, and assume that it is in non-dimensional units of mass, length, and time: the masses of the Sun, S, and Jupiter, J, are $1-\mu$ and μ, respectively, being $\mu = m_J/(m_J + m_S)$, the distance between S and J is equal to 1, and both J and S complete a revolution around their centre of mass in 2π time units. Then the mean motion of S and J becomes one, and the universal gravitation constant is also equal to one. Assume that, in these units, the planet, P, has mass μ_P and revolves around the centre of mass of S and J in a circle of radius a_P. Then, see Fig. 3, we can write the coordinates of S, J, P and of the barycentre B of the three bodies as

$$\boldsymbol{R}_S = \mathbf{M}_{\theta_1+t}\begin{pmatrix}\mu\\0\end{pmatrix}, \quad \boldsymbol{R}_J = \mathbf{M}_{\theta_1+t}\begin{pmatrix}\mu-1\\0\end{pmatrix},$$

$$\boldsymbol{R}_P = \mathbf{M}_{\theta_2+\omega_P t}\begin{pmatrix}a_P\\0\end{pmatrix}, \quad \boldsymbol{B} = \frac{\mu_P}{1+\mu_P}\boldsymbol{R}_P,$$

where $\mathbf{M}_\alpha$ is the matrix of a plane rotation of angle α, θ_1, θ_2 are the initial phases of the Sun and the planet, respectively, and ω_P is the mean motion of the planet, chosen to satisfy Kepler's third law

$$\omega_P^2\, a_P^3 = 1 + \mu_P. \tag{9}$$

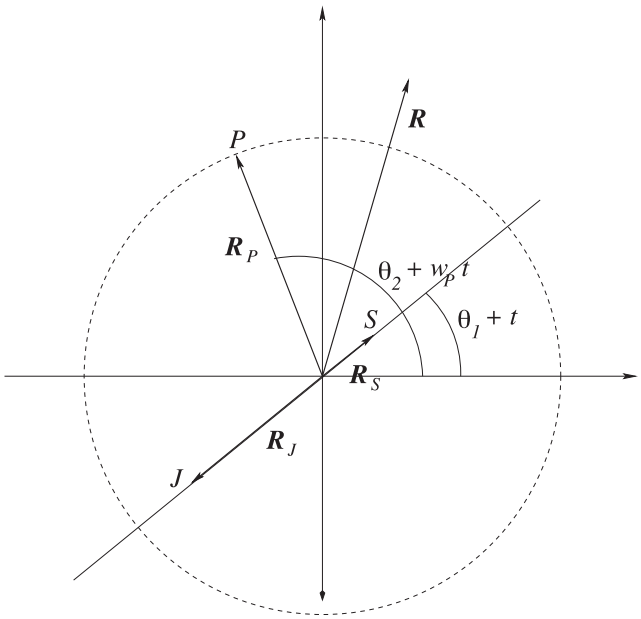

Figure 3. The geometry of the BCP, indicating the position of the Sun (S), Jupiter (J), a planet (P) and the particle (R) with respect to the centre of mass of the Sun–Jupiter.

Newton's equations for a particle (located by the position vector $\boldsymbol{R}$) submitted to the gravitational attraction of the Sun, Jupiter and the planet are

$$\ddot{\boldsymbol{R}} - \ddot{\boldsymbol{B}} = -\frac{(1-\mu)(\boldsymbol{R}-\boldsymbol{R}_S)}{\|\boldsymbol{R}-\boldsymbol{R}_S\|^3} - \frac{\mu(\boldsymbol{R}-\boldsymbol{R}_J)}{\|\boldsymbol{R}-\boldsymbol{R}_J\|^3} - \frac{\mu_P(\boldsymbol{R}-\boldsymbol{R}_P)}{\|\boldsymbol{R}-\boldsymbol{R}_P\|^3}.$$

We consider a rotating (synodical) system of coordinates, with angle $\theta_1 + t$, measured anticlockwise from the Jupiter–Sun direction (see Fig. 3). In this rotating system, the Sun and Jupiter remain fixed at $(\mu, 0)$, $(\mu - 1, 0)$, and the equations of motion for the particle (with position vector (x, y)) can be written as

$$\begin{pmatrix}\ddot{x}\\\ddot{y}\end{pmatrix} + 2\begin{pmatrix}-\dot{y}\\\dot{x}\end{pmatrix} + \begin{pmatrix}-x\\-y\end{pmatrix} - \frac{\mu_P}{a_P^2}\begin{pmatrix}-\cos\theta\\-\sin\theta\end{pmatrix} = -\frac{1-\mu}{\rho_1^3}\begin{pmatrix}x-\mu\\y\end{pmatrix} - \frac{\mu}{\rho_2^3}\begin{pmatrix}x-\mu+1\\y\end{pmatrix} - \frac{\mu_P}{\rho_P^3}\begin{pmatrix}x-a_P\cos\theta\\y-a_P\sin\theta\end{pmatrix}, \tag{10}$$

where

$$\rho_1 = ((x-\mu)^2 + y^2)^{1/2},$$

$$\rho_2 = ((x-\mu+1)^2 + y^2)^{1/2},$$

$$\rho_P = ((x-a_P\cos\theta)^2 + (y-a_P\sin\theta)^2)^{1/2},$$

$$\theta = \theta_2 - \theta_1 + t(\omega_P - 1).$$

Observe that the previous equations are a system of ODE of the form (1) with $\theta_0 = \theta_2 - \theta_1$.

Defining momenta $p_x = \dot{x} - y$, $p_y = \dot{y} + x$, the equations may be written as a Hamiltonian system of differential equations with Hamiltonian function

$$H(x, y, p_x, p_y) = \frac{1}{2}(p_x^2 + p_y^2) + yp_x - xp_y - \frac{1-\mu}{\rho_1} - \frac{\mu}{\rho_2} - \frac{\mu_P}{\rho_P} + \frac{\mu_P}{a_P^2}(y\sin\theta + x\cos\theta). \tag{11}$$

Table 1. Parameter values for the mass ratio, semimajor axis and mean motion of Saturn, Uranus and Neptune. The non-dimensional values of μ_P and a_P have been computed using the numerical values of the planetary masses and semimajor axis of the JPL ephemeris file DE405; the mean motion ω_P has been computed according to Kepler's third law (9). Suitable units are taken such that the unit of mass is the mass of the Sun–Jupiter system, the unit of distance is the Sun–Jupiter distance and the unit of time is such that Jupiter completes a revolution around the Sun in 2π units.

Planet	μ_P	a_P	ω_P
Saturn	$0.285\,613\,279\,409 \times 10^{-3}$	1.836 563 205 83	0.401 840 025 142
Uranus	$0.436\,207\,916\,533 \times 10^{-4}$	3.694 005 741 96	0.140 852 033 933
Neptune	$0.514\,647\,520\,743 \times 10^{-4}$	5.787 561 680 61	0.071 823 692 1118

In this way, we get a non-autonomous Hamiltonian system of 2 degrees of freedom which is periodic in t with period

$$T_P = \frac{2\pi}{\omega_P - 1}. \tag{12}$$

Later on, it will be useful to consider the Hamiltonian as an autonomous one. To do so, we just introduce variables t, p_t and a new Hamiltonian with 3 degrees of freedom defined by $\tilde{H}(x, y, t, p_x, p_y, p_t) = H(x, y, p_x, p_y) + p_t$.

Table 1 gives the values of the parameters corresponding to the planets of the outer Solar system used in this paper.

3.2 Dynamical substitutes of the equilibrium points

Since our aim is concerned with possible mechanisms to explain transport in the Solar system, we want to study the following possibility: the matching of the (different orbits on the) invariant manifolds of *suitable* unstable periodic orbits from different BC4BP. That is, (pseudo)-heteroclinic connections between certain periodic orbits. This section is focused on the computation of these periodic orbits.

The BR4BP may be regarded as a periodic perturbation of the RTBP. It is well known that the RTBP has five equilibrium points: the collinear ones L_1, L_2 and L_3, which are unstable (of type centre $\times$saddle) for any $\mu \in (0, 1/2]$, and the equilateral ones L_4 and L_5 that are linearly stable for $\mu \in (0, \mu_{\text{Routh}})$ and unstable for $\mu \in (\mu_{\text{Routh}}, 1/2]$. Each collinear equilibrium point L_i, $i = 1, 2, 3$ gives rise to a periodic orbit in the BR4BP. These periodic orbits are called *the dynamical substitutes* of the equilibrium points and are unstable periodic orbits. In particular, we will be interested in the role that the invariant manifolds of the dynamical substitutes of L_1 and L_2 play in the transport. We will denote them by OL_i, $i = 1, 2$. Fig. 4 shows the periodic orbits OL_1 and OL_2 – corresponding to the equilibrium points L_1 and L_2 of the Sun–Saturn RTBP – for the BR4BP Sun–Jupiter–Saturn in the synodical system of coordinates, where the Sun and Jupiter remain fixed on the x-axis.

Let us describe first how to compute these periodic orbits. We label each planet of the Solar system with the index $ip = 1, 2, 3, 4, 6, 7, 8$ corresponding to Mercury, Venus, Earth, Mars, Saturn, Uranus, Neptune, respectively. We fix ip and consider the corresponding BR4BP$_{ip}$ Sun–Jupiter–(ip planet). As has been explained in Section 2, one can take the initial phases $\theta_1 = \theta_2 = 0$. Since we look for a periodic orbit of period T_P, given by equation (12), the system to be solved is

$$F(x, y, p_x, p_y) = \boldsymbol{\phi}_{T_P}(x, y, p_x, p_y) - (x, y, p_x, p_y) = 0,$$

so (a) we need a seed to start with, and (b) we will apply Newton's method to refine it.

In order to do so, we carry out the following procedure.

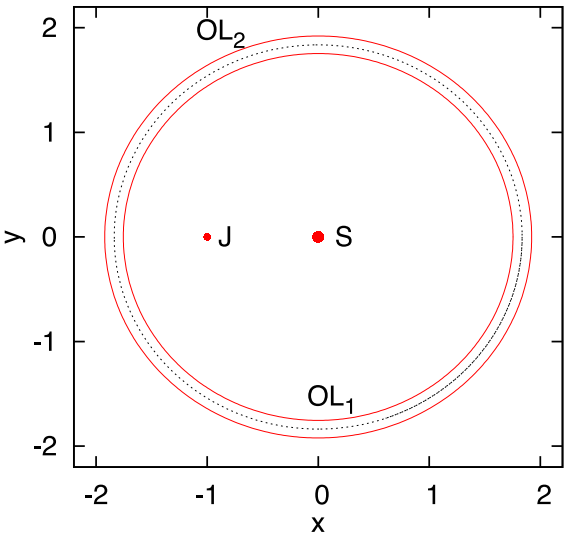

Figure 4. Projection in configuration space (rotating coordinates) of the dynamical substitutes OL_1 and OL_2 for the BR4BP Sun–Jupiter–Saturn. The orbit of Saturn is also shown with a dotted line.

(i) We consider the RTBP taking into account the Sun and the planet ip. We compute the location of the equilibrium points L_1 and L_2.

(ii) We transform the position of the L_i, $i = 1, 2$ computed to suitable units according to the BR4BP$_{ip}$ considered. Let x_{L_i} be the value of the x coordinate of the initial condition. We expect that the periodic orbit we are looking for will be close to a circular orbit of radius x_{L_i} in the BR4BP$_{ip}$ in rotating coordinates.

(iii) As an initial seed, we start with the initial condition of L_i and we apply the Newton's method to solve

$$\boldsymbol{\phi}_{T_P}(\boldsymbol{q}_0) - \boldsymbol{q}_0 = 0.$$

This is a good seed for $ip = 7, 8$ but it is not for $ip \leq 6$. Due to the high instability of the substituting periodic orbits (see Table 3), the convergence of the Newton's method fails. In these cases, the strategy is to consider a multiple shooting (MS) method. More concretely, we take as initial condition m points on the circular orbit of radius x_{L_i} and angular velocity $\omega_P - 1$. We apply Newton's method using MS and we have convergence to the required substituting periodic orbit.

As has already been said, the dynamical substitutes of L_i, $i = 1, 2$ are denoted by OL_i^{ip}, $i = 1, 2$ (or simply OL_i). In Table 2, we give the initial conditions of the dynamical substitutes OL_i, $i = 1, 2$ for the outer bicircular problems BR4BP$_{ip}$, $ip = 6, 7, 8$. The initial conditions are (x, y, p_x, p_y) with $y = p_x = 0$, so we just list (x, p_y).

The periodic orbits are of type centre $\times$ saddle, so for each one there exist stable and unstable manifolds $W^{s/u}(OL_i)$. In Table 3, we

Table 2. Initial conditions of the dynamical substitutes OL_i, $i = 1, 2$ for the outer planets.

Planet		Initial conditions (x, p_y)	
Saturn	OL_1^6	1.754 258 959 238 766,	0.704 361 873 249 9882
	OL_2^6	1.921 870 553 845 556,	0.771 909 189 593 7062
Uranus	OL_1^7	3.604 609 729 648 801,	0.507 712 919 588 7936
	OL_2^7	3.784 916 933 322 854,	0.533 110 116 817 5304
Neptune	OL_1^8	5.639 606 878 614 984,	0.405 056 738 729 9962
	OL_2^8	5.938 111 451 650 008,	0.426 496 552 726 5244

show the value of the eigenvalue $\Lambda > 1$ associated with the periodic orbits OL_i^{ip}, $i = 1, 2$ $ip = 2, \ldots, 8$. We can see that the value of the eigenvalue increases as ip decreases, and for the planets of the inner Solar system, the value of Λ is really big. This high instability is the reason why an MS method has been necessary to compute the initial conditions of the periodic orbits. In the case of Mercury, not listed in Table 3, we have found problems to compute the dynamical substitutes even using MS with a number of nodes up to 15. As Mercury is out of our scope, we have not tried to compute its dynamical substitutes with a higher number of nodes. On the other hand, due to the high instability, the linear approximation, given by equation (7), is not good enough to follow the invariant manifolds $W^{u/s}(OL_i)$ for a long time in the bicircular models corresponding to the inner planets ($ip \leq 4$).

4 CONNECTIONS BETWEEN SEQUENCES OF BICIRCULAR PROBLEMS

4.1 Invariant manifolds of OL_i^{ip}

We want to see if some natural transport mechanism in the Solar system can be explained by chaining bicircular restricted Sun–Jupiter–planet problems. In Ren et al. (2012), the authors consider *short-time natural transport* based on the existence of heteroclinic connections between libration point orbits of a pair of 'consecutive' Sun–planet RTBPs. Following the same idea, we want to explore these type of connections between two different bicircular problems.

More concretely, we want to see if the invariant manifolds of the dynamical substitutes from consecutive bicircular problems match. Notice that if two invariant manifolds of two different bicircular problems reach the same point (in position and velocity), they do not really intersect, because they are associated with different dynamic problems. But such a match is a good indicator of a possible transport mechanism in the Solar system, in the sense that could be refined to a true heteroclinic connection in a model including all the bodies involved in the two bicircular problems. We call such common points *connections*. If a connection between two bicircular problems exists, we can expect to have *natural transport* from one planet to the next one in the sequence of bicircular problems, and a particle could drift away from one planet to reach a neighbourhood of the following planet. After that, for transport between neighbourhoods of the libration points of the same Sun–planet problem, it is enough to consider an RTBP (Sun+planet+infinitesimal particle), in which case the existence of heteroclinic connections between libration point orbits around L_1 and L_2 is well known. These connections would allow a particle to continue its journey towards the innermost Solar system. See Fig. 5.

For the computation of the connections, we proceed as follows. Consider two consecutive bicircular problems $\mathrm{BR4BP}_{ip}$ and $\mathrm{BR4BP}_{ip+1}$ corresponding to the planets ip and $ip + 1$. We are interested in transits from the outer to the inner Solar system. In all the bicircular problems, OL_1 is an inner orbit than the orbit of the planet with respect to the Sun, and OL_2 is an outer orbit (see Fig. 4). Then, the suitable connections are those involving the invariant manifolds of OL_1^{ip+1} and OL_2^{ip}. It is well known that the invariant manifolds associated with the equilibrium points L_1 and L_2 in the RTBP have two branches: one goes inwards, while the other one goes outwards, at least for times not too big. The invariant manifolds of the dynamical substitutes have the same behaviour. According to this, we denote by $W_+^{u/s}(OL)$ the branch of the invariant manifold that goes outwards, and by $W_-^{u/s}(OL)$ the branch of the invariant manifold that goes inwards. See Fig. 6.

Therefore, in order to find connections, in the $\mathrm{BR4BP}_{ip}$, we compute the (linear approximation of the) parametrization of the stable manifold (see equation 7) and we follow the branch $W_+^s(OL_2)$, and in the $\mathrm{BR4BP}_{ip+1}$, we compute the (linear approximation of the) parametrization of the unstable manifold (again see equation 7) and we follow the branch $W_-^u(OL_1)$. To study if there exist connections, we also fix a section $\Sigma_R = \{(x, y); x^2 + y^2 = R^2\}$, where R is an intermediate value between the radii of the orbits of the planets of the two bicircular problems, a_{ip} and a_{ip+1}, that is $a_{ip} < R < a_{ip+1}$ (see Fig. 7).

The main objectives are: first, to determine if both manifolds reach the section Σ, and, secondly, to study which is the minimum distance between the sets $W^s(OL_2^{ip}) \cap \Sigma$ and $W^u(OL_1^{ip+1}) \cap \Sigma$. That is, we want to see if both manifolds *intersect*, or if they do not, and how far (as sets) they are from each other.

We propagate a large number of orbits along each invariant manifold and we study the evolution of the distance $r(t) = \sqrt{x^2 + y^2}$ for $|t| \leq T$, for a fixed maximum time T. First, we explore which are the maximum and minimum values of $r(t)$ that each invariant manifold $W^s(OL_2^{ip})$ and $W^u(OL_1^{ip+1})$ can reach, that are denoted by r_M and r_m. The exploration gives an idea whether the invariant manifolds can intersect and which sections Σ are more suitable. We explore in each case the behaviour of the two branches $W_\pm^{u/s}$. As we will see, the function $r(t)$ has, in general, an oscillating behaviour, but the orbits on the branch W_+, $r(t)$ take values greater than the mean radius of the corresponding orbit OL_i, whereas the orbits on the branch W_-, $r(t)$ take values less than that mean radius (at least for values of $|t|$ not too large). See Figs 8–11, where we show the evolution of $r(t)$ along both branches of some orbits of the invariant manifolds $W^{u/s}(OL_1^{ip})$ for $ip = 6, 7, 8$.

Table 3. Value of the eigenvalue $\Lambda > 1$ corresponding to the dynamical substitutes OL_i^{ip}, $i = 1, 2$ of each bicircular problem.

Outer planets	$\Lambda(OL_i^{ip})$, $i = 1, 2$	Inner planets	$\Lambda(OL_i^{ip})$, $i = 1, 2$
Neptune ($ip = 8$)	3.492, 3.286	Mars ($ip = 4$)	9×10^7, 2.5×10^8
Uranus ($ip = 7$)	14.105, 12.473	Earth ($ip = 3$)	2.8×10^7, 3.4×10^7
Saturn ($ip = 6$)	6.5×10^4, 2.5×10^4	Venus ($ip = 2$)	1.5×10^7, 1×10^7

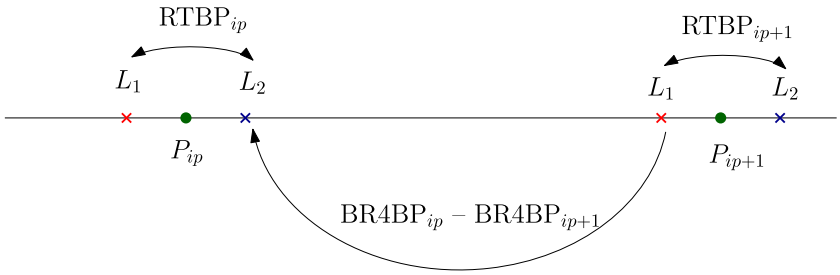

Figure 5. Scheme of the chain of connections between two consecutive restricted bicircular Sun–Jupiter–planet (BR4BP$_{ip}$) problems, and two consecutive restricted Sun–planet (P_{ip}) problems (RTBP$_{ip}$).

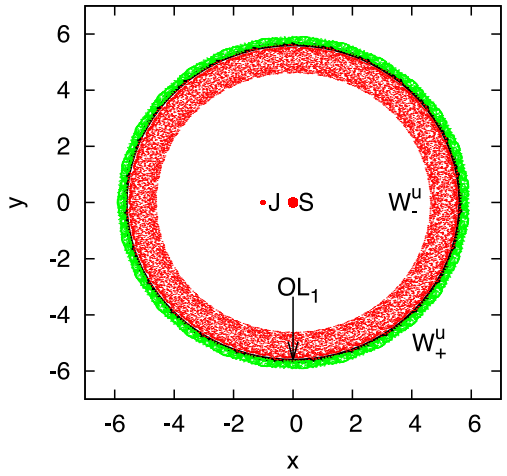

Figure 6. Projection in configuration space (rotating coordinates) of branches of the invariant manifold $W^u_+(OL^8_1)$ (outer corona) and $W^u_-(OL^8_1)$ (inner corona). The dynamical substitute OL^8_1 is the periodic orbit between the two branches. See the text for further details and also Fig. 8.

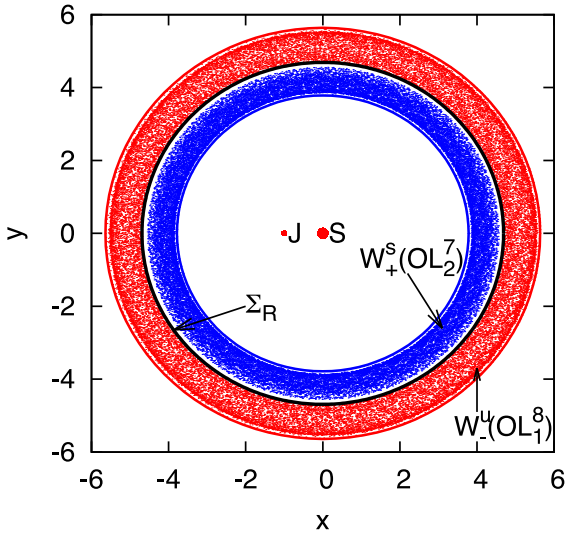

Figure 7. Projection in configuration space (rotating coordinates) of the dynamical substitutes OL^8_1, OL^7_2, one orbit on the invariant manifolds $W^u(OL^8_1)$ and $W^s(OL^7_2)$, and the section Σ_R for $R = \sqrt{22}$.

It seems natural that the branches to be considered, in order to see if the invariant manifolds $W^u(OL^{ip+1}_1)$ and $W^s(OL^{ip}_2)$ match, should be W^u_- and W^s_+. Figs 8 and 9 suggest that this is the case for Uranus and Neptune. Notice that in the BR4BP$_8$ there are orbits on the $W^u_+(OL^8_1)$ branch that, after some time moving outwards (with $r(t)$ greater than the mean radius of OL^8_1), cross the OL^8_1 orbit and move inwards (see Fig. 8, left). This can be explained in two ways: on one hand, the orbits follow paths that overlap the orbit of the planet, so the particle can have a close encounter with the planet and suffer a big deviation; on the other hand, the existence of homoclinic orbits to OL^8_1 would allow the existence of transit orbits, i.e. orbits that spend some time surrounding the planet, have a passage near the OL^8_1 orbit and follow a path to the inner region (this behaviour has been observed in the RTBP, see for example Barrabés, Mondelo & Ollé 2009). Nevertheless, as Fig. 9 suggests, this behaviour is rare. In this paper, we only consider the branches $W^u_-(OL^8_1)$ and $W^s_+(OL^7_2)$ for a possible matching.

We repeat the exploration for the orbits on the manifold $W^u(OL^7_1)$ (Sun–Jupiter–Uranus problem) and $W^s(OL^6_2)$ (Sun–Jupiter–Saturn problem), see Figs 10 and 11. In the last case, the orbits OL^6_i are highly unstable (see Table 3) and the invariant manifolds spread far away (inwards and outwards). That is the particular case of the branch $W^s_-(OL^6_2)$: although their orbits initially tend to the inner Solar system, most of them move outwards reaching distances $r(t)$ greater than the location of Neptune (see Fig. 11, right).

In Table 4, we summarize the maximum and minimum values of $r(t)$ of each manifold for $|t| \leq 10^4$. As we have explained, we are exploring transport in the outer Solar system, and we have not studied from Saturn inwards. This minimum and maximum values indicate that there exists the possibility of a connection between the bicircular problems for Uranus and Neptune and Saturn and Uranus.

4.2 Matching consecutive bicircular problems

Next we choose two intermediate sections Σ_R, for $R = R_1 = \sqrt{22}$ and $R = R_2 = \sqrt{11}$, and we compute the intersection of the appropriate invariant manifolds with the sections: on one hand $W^u(OL^8_1) \cap \Sigma_{R_1}$ and $W^s(OL^7_2) \cap \Sigma_{R_1}$, to explore connections between the bicircular problems Sun–Jupiter–Neptune and Sun–Jupiter–Uranus, and, on the other hand, between $W^u(OL^7_1) \cap \Sigma_{R_2}$ and $W^s(OL^6_2) \cap \Sigma_{R_2}$ to explore connections between the bicircular problems Sun–Jupiter–Uranus and Sun–Jupiter–Saturn.

First, we compute the value of the osculating semimajor axis at each point of the orbits of the invariant manifolds at the section, in order to obtain an equivalent of Fig. 1 for the bicircular problem, see Fig. 12. In the case of the bicircular problems associated with Neptune and Uranus, we see that there are points of both invariant manifolds with the same semimajor axis, and this suggests the existence of intersections between these manifolds. In the case of Saturn and Uranus bicircular problems, it seems that there are not common points for $|t| < 10^4$.

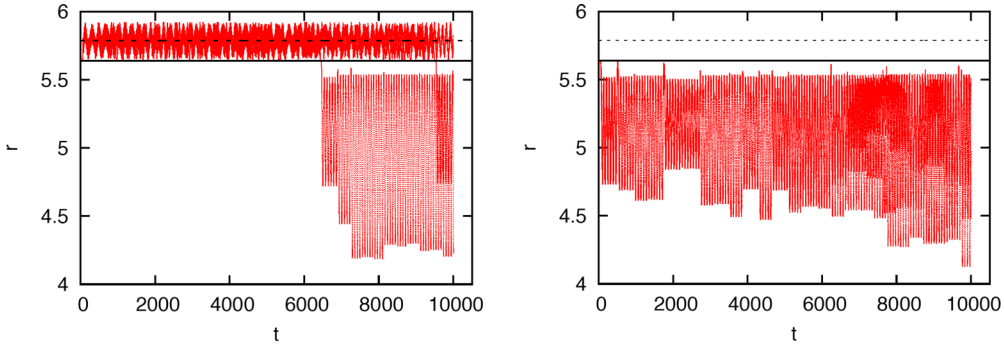

Figure 8. Behaviour of the distance $r(t)$ of some orbits of the branches $W^u_+(OL^8_1)$ (left) and $W^u_-(OL^8_1)$ (right). The dotted line corresponds to $r = a_8$, the circular orbit of Neptune. The continuous black line corresponds to the value of r of the orbit OL^8_1.

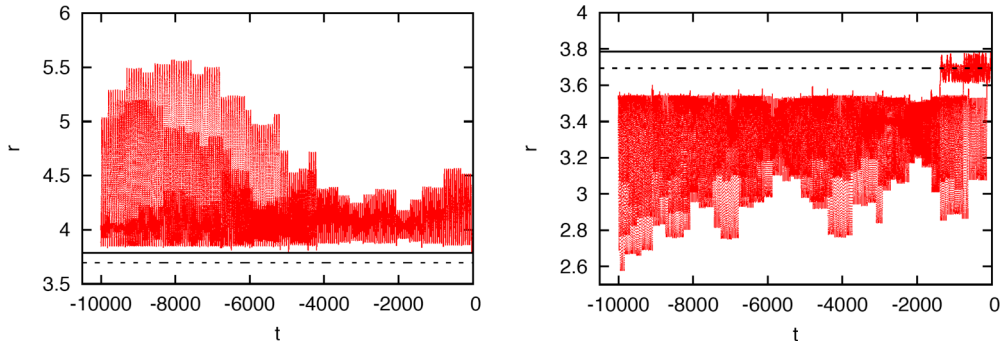

Figure 9. Behaviour of the distance $r(t)$ of some orbits of the branches $W^s_+(OL^7_2)$ (left) and $W^s_-(OL^7_2)$ (right). The dotted line corresponds to $r = a_7$, the circular orbit of Uranus. The continuous black line corresponds to the value of r of the orbit OL^7_2.

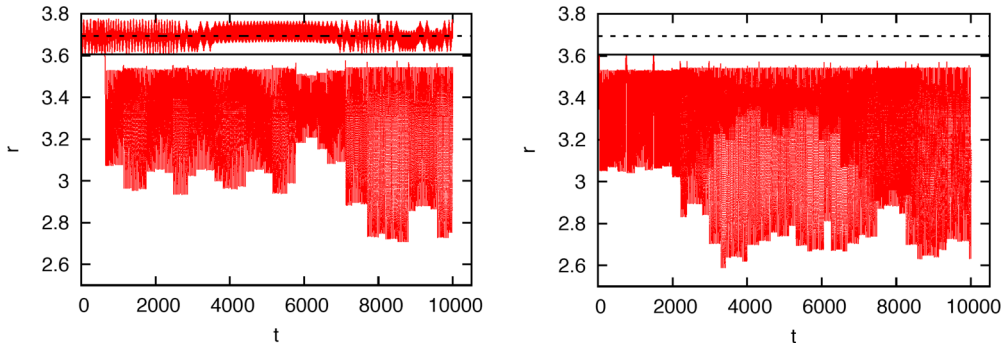

Figure 10. Behaviour of the distance $r(t)$ of some orbits of the branches $W^u_+(OL^7_1)$ (left) and $W^u_-(OL^7_1)$ (right). The dotted line corresponds to $r = a_7$, the circular orbit of Uranus. The continuous black line corresponds to the orbit OL^7_2.

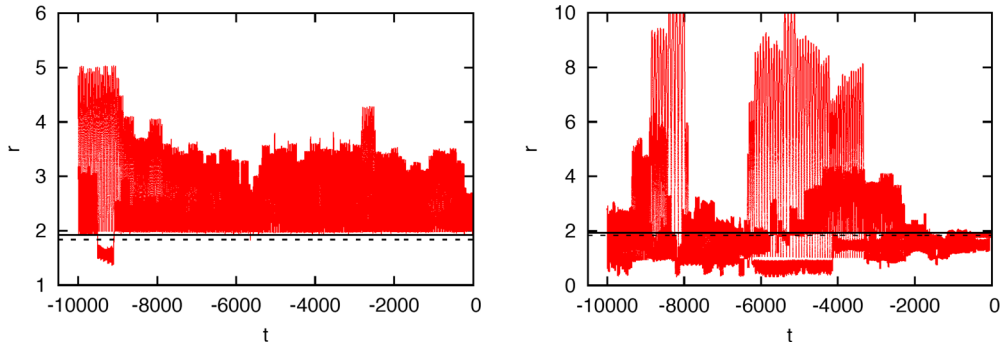

Figure 11. Behaviour of the distance $r(t)$ of some orbits of the branches $W^s_+(OL^6_2)$ (left) and $W^s_-(OL^6_2)$ (right). The dotted line corresponds to $r = a_6$, the circular orbit of Saturn. The continuous black line corresponds to the orbit OL^6_2.

Table 4. Minimum and maximum values of $r(t)$ of each manifold $W^u(OL_1)$ and $W^s(OL_2)$ (resp) and $|t| \leq 10^4$.

Bicircular problem	$r_m(W^u(OL_1^{ip}))$	$r_M(W^s(OL_2^{ip}))$
Sun–Jupiter–Neptune ($ip = 8$)	4.096 29	
Sun–Jupiter–Uranus ($ip = 7$)	2.606 07	5.572 42
Sun–Jupiter–Saturn ($ip = 6$)		>10

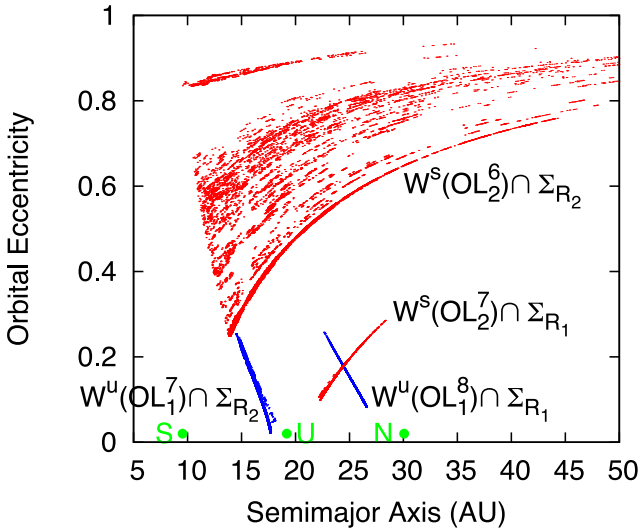

Figure 12. Osculating semimajor axis versus eccentricity for the points of $W^u(OL_1^8) \cap \Sigma_{R_1}$ and $W^u(OL_1^7) \cap \Sigma_{R_2}$, and $W^s(OL_2^7) \cap \Sigma_{R_1}$ and $W^s(OL_2^6) \cap \Sigma_{R_2}$.

In order to look for actual intersections, we explore the distance between the sets $W^u(OL_1^{ip+1}) \cap \Sigma_R$ and $W^s(OL_2^{ip}) \cap \Sigma_R$. We proceed in the following way. We take N initial conditions of N orbits along each invariant manifold, according to formula (7), follow these orbits and compute their intersections with the section Σ_R for $|t| < T$, for a fixed T (so this means a finite time of integration along each orbit). As we have seen in Figs 8 and 9, the distance $r(t)$ from the orbits to the origin has an oscillatory behaviour so, in general, the orbits meet the section several times. Each orbit on the invariant manifold is uniquely determined by the parameter θ [see equation (7) for more details]. Thus, each point on the intersection $W^u(OL_1^{ip+1}) \cap \Sigma_R$ is determined by θ and the time required to reach the section, t_Σ. Then, for each one of these points (θ, t_Σ), we compute the distance in position and velocity to each point on the set $W^s(OL_2^{ip}) \cap \Sigma_R$. We keep both the minimum distance in position, denoted as $d_p(\theta, t_\Sigma)$, and the minimum distance in velocity, denoted as $d_v(\theta, t_\Sigma)$. A connection between the bicircular problems ip and $ip + 1$ would be obtained if $d_p + d_v = 0$.

We start with BR4BP$_7$ and BR4BP$_8$, and their intersections with the section Σ_{R_1}. We are focused on *short-term integrations*, so for the explorations done we take $N = 500$ and $T = 10^4$ (although of course the Solar system is a lot older). We do not find any connection, in the sense that $d_p + d_v$ is never exactly zero. Fig. 13 shows the results obtained in this case. The plot on the left shows that there exist points such that their distance d_p is less than 10^{-7}, and few points with distance of the order of 10^{-9} (about 800 m). The plot on the right shows the distance in velocity d_v only for those points such that $d_p < 10^{-5}$. In this case, we observe that $d_v > 10^{-5}$, and there are some points such that $d_v \in (10^{-4}, 10^{-3})$ (10^{-5} is about 1.306 m s^{-1}).

Next we repeat the exploration to look for connections between the bicircular problems Sun–Jupiter–Uranus (BR4BP$_7$) and Sun–Jupiter–Saturn (BR4BP$_6$). Similarly to the previous case, initially we consider the branches $W^u_-(OL_1^7)$ (inner branch, see Fig. 10, right) and $W^s_+(OL_2^6)$ (outer branch, see Fig. 11, left). We follow $N = 500$ orbits up to the section Σ_{R_2} for $|t| < 10^4$. The results are shown in Fig. 14. We obtain similar results as in the previous case in positions (minimum d_p of the order of 10^{-8} or 10^{-9}), but the results in velocities are not so good. We remark that the simulations have been done for a fixed and moderate value of T ($T = 10^4$). Of course, for higher values of T – *long-term* integrations – we might have better results. This is the case for the bicircular problems Sun–Jupiter–Uranus (BR4BP$_7$) and Sun–Jupiter–Saturn (BR4BP$_6$) where we obtain minimum in distance d_p of the order of 10^{-8} and minimum in velocities d_v of the order of 10^{-3} for $T = 5 \times 10^4$.

Recovering the behaviour of the branches of $W^s(OL_2^6)$, we notice that the 'inner' branch W^s_- has a significant number of orbits that move outwards after some time (see Fig. 11, right). In fact, this branch sweeps a wide region of the outer Solar system, and a possible connection with the branches of $W^u(OL_1^7)$ can occur. Therefore, we repeat the exploration with the $W^s_-(OL_2^6)$ branch: we compute its intersections with the section Σ_{R_2} and then we look for matchings with $W^u_-(OL_1^7) \cap \Sigma_{R_2}$. The results are shown in Fig. 15. Again in positions we have good results (points at a distance of orders of metres), but in velocities the differences are larger than in the previous case.

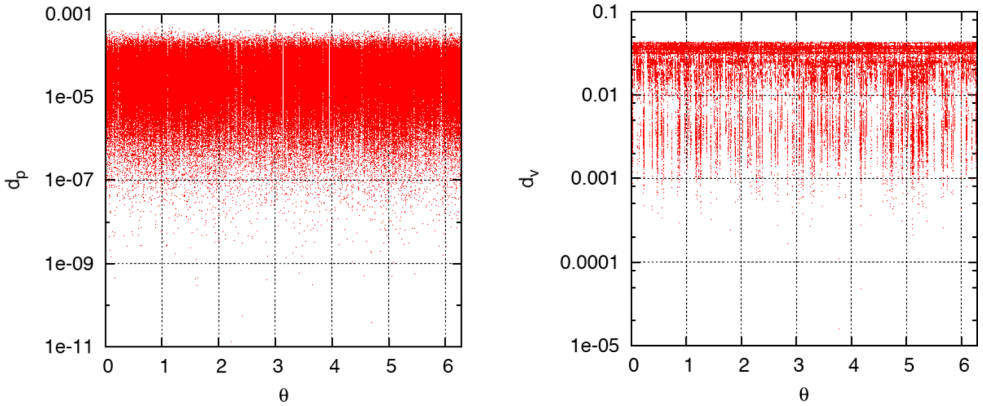

Figure 13. Minimum distances d_p (positions, left) and d_v (velocities, right) between points of the invariant manifolds at the section Σ_{R_1} of the Uranus and Neptune bicircular problems. See the text for more details.

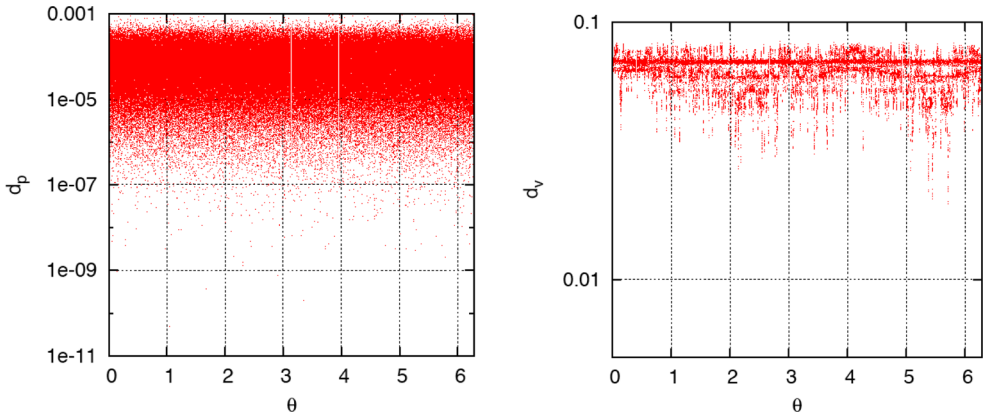

Figure 14. Minimum distances d_p (position, left) and d_v (velocities, right) between points of the invariant manifolds $W^u_-(OL^7_1)$ and $W^s_+(OL^6_2)$ at the section Σ_{R_2}.

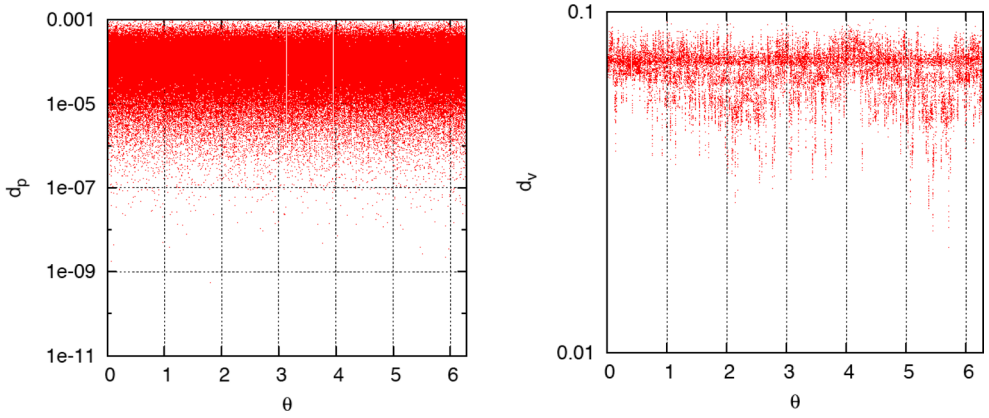

Figure 15. Minimum distances d_p (position, left) and d_v (velocities, right) between points of the invariant manifolds $W^u_-(OL^7_1)$ and $W^s_-(OL^6_2)$ at the section Σ_{R_2}.

5 CONCLUSIONS

In this paper, we have explored a natural transport mechanism, in the outer region of the Solar system, based on the existence of heteroclinic connections between the invariant hyperbolic manifolds of the dynamical substitutes of the collinear libration points of the Sun–Neptune, Sun–Uranus and Sun–Saturn RTBPs. The study is based on the analysis of a sequence of BR4BPs, in which, aside from the Sun and the three outer planets already mentioned, the gravitational effect of Jupiter is included in all the bicircular problems. The existence of connections between the manifolds of the Sun–Jupiter–Neptune and Sun–Jupiter–Uranus suggests a natural *short-term* mass transport mechanism between these two systems. The situation is not so clear between the Sun–Jupiter–Uranus and Sun–Jupiter–Saturn, since the invariant manifolds considered for the short-term transport do not have a clear intersection. However, integration for longer ranges of time seems to be a good strategy to improve such connections. Of course, the ellipticity of the actual planet orbits and additional perturbations of the other planets and forces, as well as collisional processes should also be taken into account for a more accurate description of transport mechanisms.

The paper includes a rigorous justification of the procedures used for the computations of the periodic orbits and their associated invariant manifolds in the bicircular restricted problems.

ACKNOWLEDGEMENTS

This work has been supported by the Catalan grants 2014 SGR 1145 (GG and EB), 2014 SGR 504 (MO), and the Spanish grants MTM2013-41168-P (GG, EB, JMM), MTM2014-52209-C2-1-P (JMM) and MCyT/FEDER2015-65715-P (MO).

REFERENCES

Andreu M. A., 1998, PhD thesis, Univ. Barcelona
Barrabés E., Mondelo J. M., Ollé M., 2009, Nonlinearity, 22, 2901
Bollt E. M., Meiss J. D., 1995, Phys. Lett. A, 204, 373
Gladman B. J., Burns J. A., Duncan M., Lee P., Levison H. F., 1996, Science, 271, 1387
Gómez G., Jorba A., Masdemont J. J., Simó C., 1993, Celest. Mech. Dyn. Astron., 56, 541
Lo M. W., Ross S., 1999, New Technology Report NPO-20377
Ollé M., Barrabés B., Gómez G., Mondelo J. M., 2015, in Corbera M., Cors J. M., LLibre J., Koroveinikov J., eds., Proc. Hamiltonian Systems and Celestial Mechanics, Research Perspectives CRM, Barcelona, p. 45
Ren Y., Masdemont J. J., Gómez G., Fantino E., 2012, Commun. Nonlinear Sci. Numer. Simul., 17, 844

APPENDIX A

The lemmas in this appendix support the statements in Section 2.

Lemma 2 *The function* $\boldsymbol{\varphi}(\theta)$, *as defined in* equation (4), *is* 2π-*periodic in* θ *and satisfies the invariance equation* (5).

Proof: The invariance equation is proven by the following calculation, for which it is necessary to use Lemma 1 in the second equality:

$$\boldsymbol{\phi}_t^\theta\left(\boldsymbol{\varphi}(\theta)\right) = \boldsymbol{\phi}_t^\theta\left(\boldsymbol{\phi}^{\theta_0}_{(\theta-\theta_0)/\omega}(\boldsymbol{x}_0)\right) = \boldsymbol{\phi}^{\theta_0}_{t+(\theta-\theta_0)/\omega}(\boldsymbol{x}_0) = \boldsymbol{\varphi}(\theta+t\omega).$$

A similar argument proves 2π-periodicity:

$$\boldsymbol{\varphi}(\theta+2\pi) = \boldsymbol{\phi}^{\theta_0}_{2\pi/\omega+(\theta-\theta_0)/\omega}(\boldsymbol{x}_0) = \boldsymbol{\phi}^{\theta_0+2\pi}_{(\theta-\theta_0)/\omega}\Big(\underbrace{\boldsymbol{\phi}^{\theta_0}_{2\pi/\omega}(\boldsymbol{x}_0)}_{\boldsymbol{x}_0}\Big) = \boldsymbol{\varphi}(\theta),$$

and the lemma follows. □

Lemma 3 *The function* $\boldsymbol{v}(\theta)$ *defined in* equation (6) *is* 2π-*periodicin* θ *and satisfies*

$$D\boldsymbol{\phi}_t^\theta\Big(\boldsymbol{\varphi}(\theta)\Big)\boldsymbol{v}(\theta) = \Lambda^{t/T}\boldsymbol{v}(\theta+t\omega). \tag{A1}$$

Proof: We first prove equation (A1). Using the definition of $\boldsymbol{v}$, the chain rule and Lemma 1,

$$\begin{aligned} D\boldsymbol{\phi}_t^\theta\left(\boldsymbol{\varphi}(\theta)\right)\boldsymbol{v}(\theta) &= D\boldsymbol{\phi}_t^\theta\left(\boldsymbol{\phi}^{\theta_0}_{(\theta-\theta_0)/\omega}(\boldsymbol{x}_0)\right)\Lambda^{-\frac{\theta-\theta_0}{2\pi}} D\boldsymbol{\phi}^{\theta_0}_{(\theta-\theta_0)/\omega}(\boldsymbol{x}_0)\boldsymbol{v}_0 \\ &= \Lambda^{-\frac{\theta-\theta_0}{2\pi}} D\Big(\boldsymbol{\phi}_t^\theta \circ \boldsymbol{\phi}^{\theta_0}_{(\theta-\theta_0)/\omega}\Big)(\boldsymbol{x}_0)\boldsymbol{v}_0, \\ &= \Lambda^{\frac{t\omega}{2\pi}}\Lambda^{-\frac{\theta+t\omega-\theta_0}{2\pi}} D\boldsymbol{\phi}^{\theta_0}_{(\theta+t\omega-\theta_0)/\omega}(x_0)v_0 \\ &= \Lambda^{t/T}\boldsymbol{v}(\theta+t\omega). \end{aligned}$$

A similar argument proves 2π-periodicity in θ,

$$\begin{aligned} v(\theta+2\pi) &= \Lambda^{-\frac{\theta+2\pi-\theta_0}{2\pi}} D\boldsymbol{\phi}^{\theta_0}_{(\theta+2\pi-\theta_0)/\omega}(\boldsymbol{x}_0)\boldsymbol{v}_0 \\ &= \Lambda^{-\frac{\theta+2\pi-\theta_0}{2\pi}} D\Big(\boldsymbol{\phi}^{\theta_0+2\pi}_{(\theta-\theta_0)/\omega}\circ\boldsymbol{\phi}^{\theta_0}_{2\pi/\omega}\Big)(\boldsymbol{x}_0)\boldsymbol{v}_0 \\ &= \Lambda^{-1}\Lambda^{-\frac{\theta-\theta_0}{2\pi}} D\boldsymbol{\phi}^{\theta_0+2\pi}_{(\theta-\theta_0)/\omega}\Big(\underbrace{\boldsymbol{\phi}^{\theta_0}_{2\pi/\omega}(\boldsymbol{x}_0)}_{\boldsymbol{x}_0}\Big)\underbrace{D\boldsymbol{\phi}_T^{\theta_0}(\boldsymbol{x}_0)\boldsymbol{v}_0}_{\Lambda\boldsymbol{v}_0} \\ &= v(\theta), \end{aligned}$$

and the lemma follows. □

Lemma 4 *The expression* (7) *of the linear approximation of an invariant manifold of a periodic orbit satisfies the approximate invariance equation* (8).

Proof: Expanding $\boldsymbol{\phi}_t^\theta$ by Taylor around $\boldsymbol{\varphi}(\theta)$, and using Lemmas 2 and 3, we have

$$\begin{aligned} \boldsymbol{\phi}_t^\theta\Big(\bar{\boldsymbol{\psi}}(\theta,\xi)\Big) &= \boldsymbol{\phi}_t^\theta\Big(\boldsymbol{\varphi}(\theta)\Big) + D\boldsymbol{\phi}_t^\theta\Big(\boldsymbol{\varphi}(\theta)\Big)\xi\,\boldsymbol{v}(\theta) + O(\xi^2) \\ &= \boldsymbol{\varphi}(\theta+t\omega) + \xi\,\Lambda^{t/T}\boldsymbol{v}(\theta+t\omega) + O(\xi^2), \end{aligned}$$

and the lemma follows. □

This paper has been typeset from a TEX/LATEX file prepared by the author.